E3S Web of Conferences **730**, 02006 (2026) https://doi.org/10.1051/e3sconf/202673002006
Soft Soils 2026

The influence of suction and density on the resilient modulus of undercompacted soils

Aditi Rana[1*], *Arash* Azizi[2], *Malcolm* Whitworth[1], *Marti* Lloret-Cabot[3], and *David* Geoffrey Toll[3]

[1] School of Environmental and Life Sciences, University of Portsmouth, UK
[2]James Watt School of Engineering, University of Glasgow, UK
[3]School of Engineering, Durham University, UK

Abstract. The resilient modulus is a key parameter in road and railway subgrade design, reflecting soil stiffness under repeated loading. While subgrades are typically compacted to maximum dry density, many existing infrastructures are supported by soils with densities lower than the maximum due to inadequate compaction or long-term density loss. Understanding the behaviour of these undercompacted and often unsaturated soils is therefore essential for both infrastructure assessment and design. This paper reviews the influence of cyclic stress, suction, density, and drying–wetting cycles on the resilient modulus of four unsaturated soils with high fines content using experimental data from the literature. The analysis indicates that resilient modulus increases with suction but decreases with increasing cyclic stress for these soils. Resilient modulus is also found to decrease significantly with reductions in density at all suction levels. Moreover, drying–wetting cycles were observed to cause soil deterioration, leading to stiffness degradation and a reduction in resilient modulus of the soil examined. A review of several predictive models showed that neglecting the influence of density and drying-wetting cycles results in weaker agreement between model predictions and experimental observations. To address these limitations, a new model is proposed that incorporates the effects of density variations and soil deterioration due to drying–wetting cycles, leading to improved predictions of the resilient modulus for undercompacted soils.

1 Introduction

The resilient modulus M_R of subgrade soils is a fundamental property in the design of roads and railways, as it quantifies the material's ability to recover and withstand under repeated traffic loading [1-3]. It is determined experimentally using the cyclic triaxial test, in which a cylindrical soil specimen is subjected to a cyclic deviator stress under a constant confining pressure, and MR is calculated as the ratio of the applied cyclic deviator stress to the recoverable axial strain [1].In practice, subgrades are typically compacted at maximum dry density, $\rho_{d,max}$ to achieve high stiffness and stability [2]. However, a significant proportion of existing infrastructure is supported by soils that were either compacted below their maximum dry density due to substandard compaction or have experienced a gradual loss of density over time due to seasonal moisture fluctuations and long-term traffic loads [4,5]. Understanding the mechanical behaviour of these "undercompacted" soils, is therefore essential for both the assessment of existing infrastructure and the realistic design of new construction.

The mechanical response of these unsaturated undercompacted soils is governed by a complex interaction between their compaction state and water retention properties, namely, suction and degree of saturation. Soils under unsaturated conditions tend to exhibit higher stiffness and strength, especially at lower values of degree of saturation, S_r (and corresponding high values of suction, s) [6]. The magnitude of this effect is regulated by S_r, which governs the distribution and effectiveness of pore water menisci within the soil fabric [7]. The degree of saturation is related to suction through the soil water retention curve, which, in addition depends on soil's dry density, ρ_d [8-11]. Consequently, a comprehensive framework for predicting M_R must simultaneously account for the stress state of the soil, the water retention behaviour, and its initial compaction state.

Although numerous models have been proposed to predict MR for unsaturated soils, they are often calibrated for conditions at maximum dry density and assume no explicit account of dry density in their formulation [12,13,19,20]. This assumption reduces their ability to represent M_R, particularly for undercompacted soils. Accordingly, this study aims to (1) systematically analyse the factors controlling M_R at compaction states below maximum dry density; (as a representative state of undercompacted soils), and (2) develop an enhanced model for unsaturated soils that explicitly accounts for the effects of undercompaction.

* Corresponding author: aditi.rana@myport.ac.uk

2 Material

2.1 Soil index properties

Experimental data for four subgrade soils were compiled from independent published studies [14–17]: MTCS (Mixed Two Commercial Soils), GC (Guangdong Clay), SM (Silty Sand), and CSF (Clay Subgrade Filler). These soils contain substantial fine fractions and were tested at dry densities, ρ_d below their maximum dry density, $\rho_{d,\max}$, representing undercompacted states; except for GC which includes also data compacted at $\rho_{d,\max}$, allowing comparison across varying density conditions. Their index properties are summarised in Table 1.

Table 1. Index properties of the selected soils.

Soil properties	MTCS [14]	CSF [17]	GC [15]	SM [16]
Sand (%)	48.0	4.6	46.5	61.0
Silt (%)	46.0	76.2	53.6*	39.0*
Clay (%)	6.0	19.2		
LL (%)	-	46.1	42.0	18.0
PI (%)	-	23.7	19.1	3.7
G_s	2.72	2.73	3.2	2.64
OMC (%)	16.50	20.41	12.50	8.50
$\rho_{d,max}$ (Mg/m^3)	1.66	1.64	1.89	2.08
ρ_d (Mg/m^3)	1.57	1.47;1.55	1.89;1.79; 1.70;1.60	1.98

Notes: * Indicates combined silt and clay fractions. G_s = specific gravity; *LL*= liquid limit; *PI* = plasticity index; OMC= optimum moisture content; ρ_d = dry density; $\rho_{d,max}$ = maximum dry density.

2.2 Water retention properties

The soil water retention curves (SWRCs) for the selected soils are also available, but they are presented later in the next discussion section. The SWRC for MTCS and SM were obtained on samples near their maximum dry density (1.98 Mg/m^3 and 1.57 Mg/m^3). In contrast, GC was tested at varying dry densities, and CSF at a dry density of 1.47 Mg/m³ and 1.55 Mg/m³. The experimental data were fitted using the Fredlund and Xing [18] model to provide a clearer representation of the SWRC shape over a wide range of suctions.

3 Discussion

The compiled experimental dataset was analysed to identify the fundamental factors governing M_R, with particular emphasis on the effects of cyclic stress, water retention characteristics, and dry density.

3.1 Effect of cyclic deviatoric stress on M_R

Fig. 1 a-c show the variation of M_R with cyclic deviatoric stress, q_{cyc}. Data for MTCS is not presented here as the tests on this soil were carried out at constant q_{cyc}. M_R for all soils decreases consistently with increasing q_{cyc}. This reduction in stiffness, observed at constant suction, is attributed to the inability of the fine matrix (silt and clay) to sustain suction-induced bonding (menisci) under increasing cyclic loading. As q_{cyc} increases, progressive local degradation of the suction bonding within the soil occurs, leading to a corresponding loss of stiffness.

This stiffness degradation is observed at both low and high suctions, with the exception of SM at suction of 10 kPa (Fig. 1a), where M_R appears to remain relatively unchanged. Overall, the degradation is slightly more pronounced at higher suction levels. For example, in the case of GC, M_R decreases with increasing cyclic stress by about 25% at a suction of 821 kPa, whereas at a suction of 10 kPa, it decreases by about 20%. This behaviour indicates a greater deterioration of the soil (i.e., greater loss of particle bonding) at elevated suctions, which typically affects more the fine-aggregated matrix.

3.2 Effect of suction on M_R

Fig. 2 shows the variation of the resilient modulus with suction for MTCS, SM, and GC, with the corresponding degree of saturation indicated as labels. The soil water retention curves (SWRCs) for these soils are also presented on a secondary (vertical, right) axis in terms of S_r.

For each soil, the specimens were prepared at similar void ratios, as they were compacted at, or very close to, their maximum dry density. During cyclic loading, although some permanent accumulated strain may have developed, the strains were very small; hence, the change in void ratio is expected to be minimal and unlikely to significantly affect the observed influence of cyclic loading. M_R exhibits a nonlinear increase with increasing matric suction and decreasing degree of saturation (Fig. 2a-c). This behaviour is characterised by a relatively modest increase in M_R at lower suction ranges, followed by a more rapid increase at higher suction levels (note that suction on the x-axis is plotted on a logarithmic scale).

Closer inspection of Fig. 2 shows a distinct inflection point that approximately aligns with the soil air entry value (AEV) of the SWRC, marking the transition from saturated to unsaturated conditions. At suctions below the AEV, water losses occur at larger pores a slight influence to increase soil stiffness. Once suction exceeds the AEV, the removal of water occurs at smaller intra-aggregate pores which leads to a more pronounced effect on the increase of soil's stiffness.

The influence of q_{cyc} on the M_R measured for SM and GC is evident in Fig. 2b and c. An increase in q_{cyc} leads to a reduction in M_R, as discussed previously, and additionally causes a gradual slight shift to high suctions of the transition and inflection point of the $M_R - \log s$ curves. This may suggest that higher cyclic stresses reduce the effectiveness of suction-related bonding (or the menisci) at lower suction levels, so greater suction is required to produce the same stiffening effect.

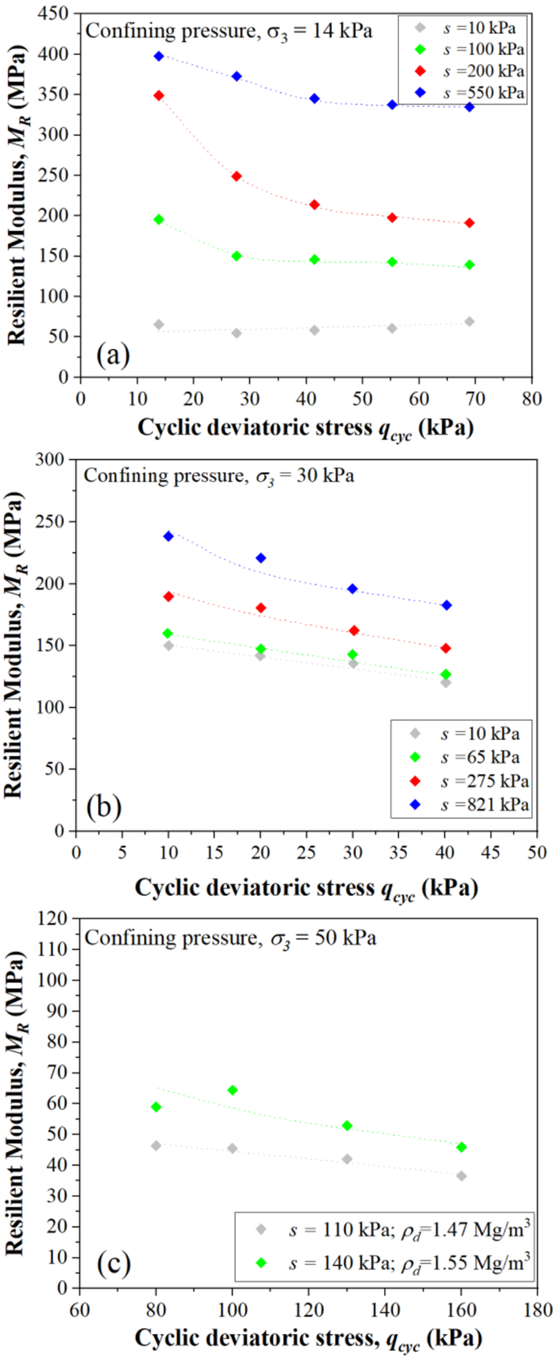

Fig. 1. Variation of resilient modulus with cyclic deviatoric stress (a) SM (b) GC (c) CSF.

3.3 Effect of dry density on M_R

Fig. 3 shows the influence of compaction dry density on M_R of GC. As the initial dry density decreases, M_R also decreases, confirming that a less compacted soil structure results in lower stiffness. In addition to the reduction in M_R, the inflection points of $M_R - \log s$ curves shift toward higher suction levels with decreasing dry density. The soil water retention curves for GC at varying dry density levels are also presented in Fig. 3, whereby the AEV decreases as dry density decreases. In general, this results in a shift of the SWRCs toward lower suction levels (except for ρ_d = 1.70 Mg/m³, see Fig. 3).

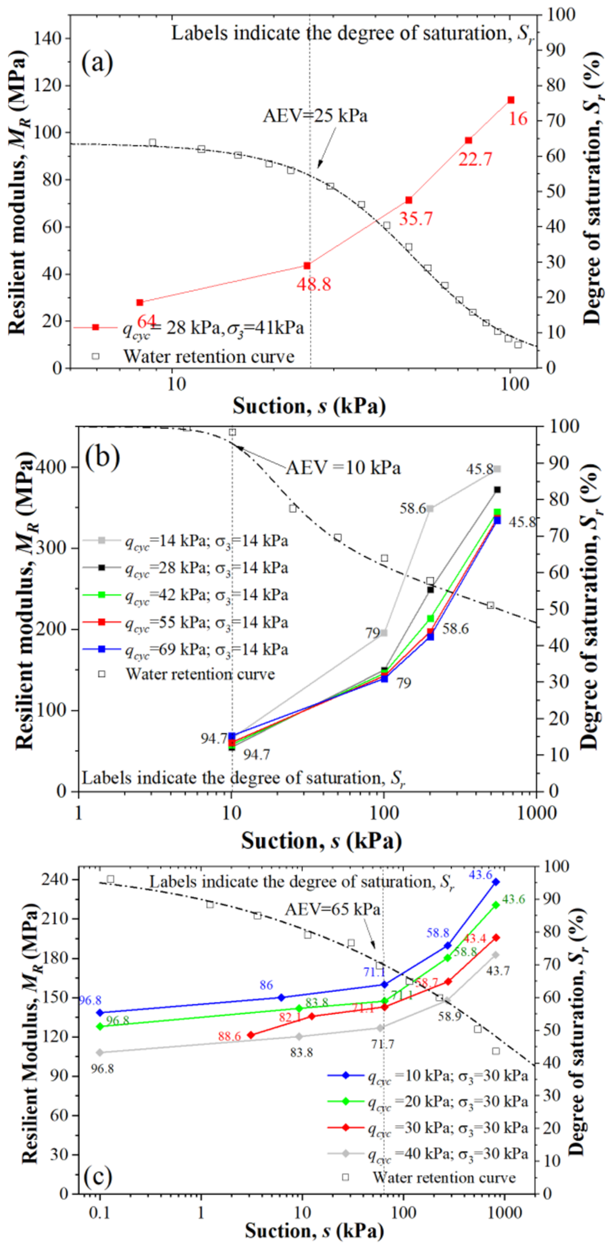

Fig. 2. Variation of resilient modulus with water retention properties (a) MTCS (b) SM (c) GC.

The observed trends can be explained by different physical mechanisms associated with soil structure. As density decreases, the soil fabric becomes progressively looser, resulting in larger pore sizes and a reduction in capillary resistance to air entry. Consequently, the AEV decreases and the soil water retention curve shifts toward lower suction levels. In contrast, the inflection point in the $M_R - \log s$ curve reflects the suction level at which suction-induced bonding at particle contacts becomes sufficient to significantly enhance soil stiffness. In looser soils, where particle contacts are less effective, higher suction levels are required to mobilise these capillary forces and contribute to stiffness enhancement, leading to a shift of the inflection point toward higher suction levels.

The effect of decreasing dry density on M_R exhibit a response similar to that produced by increasing q_{cyc}. In both cases, the effective contribution of the soil skeleton to overall stiffness is reduced, either due to a looser fabric (lower dry density) or due to progressive degradation of interparticle contacts under higher cyclic loading. As the soil structure becomes less effective in resisting deformation, a greater level of suction is required to mobilise capillary forces at particle contacts and compensate for the loss of mechanical interlocking.

The observed density effect for GC was attributed to variations in initial density at the time of compaction. However, variations in soil structure and density can also arise as a result of drying–wetting cycles, particularly if soil specimens are undercompacted. In the case of CSF (Fig. 4), tests were conducted at two initial dry densities, 1.47 Mg/m3 and 1.55 Mg/m3, with specimens subjected to drying–wetting cycles, ranging from one to six cycles. Following cycles, specimens were tested at a suction of 110 kPa and 140 kPa, respectively.

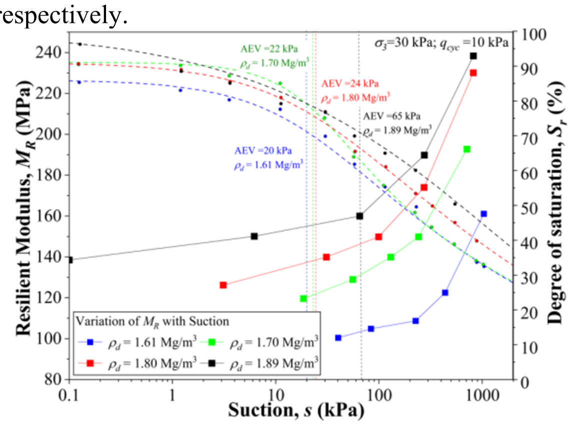

Fig. 3. Effect of initial density on the soil-water retention curve and resilient modulus for GC.

Fig. 4a presents M_R of CSF subjected to different numbers of drying-wetting cycles. When specimens are compared at the same number of cycles, M_R is higher for samples with slightly higher density, an effect that is further enhanced by the application of higher suction. However, when specimens tested at the same suction level are examined, an opposite trend is observed. Although density increases with drying-wetting cycles due to strain accumulation, M_R decreases as the number of cycles increases. This indicates that dry density alone is not the governing factor controlling stiffness of CSF, as repeated drying–wetting cycles progressively deteriorate the soil fabric and weaken interparticle contacts, leading to a reduction in resilient modulus.

Fig. 4b illustrates the primary SWRCs of CSF for specimens as well as following successive drying–wetting cycles. The second drying SWRC for both specimens shows a pronounced increase in water retention capacity, with the curves shifting towards higher suction levels. This behaviour corresponds to an increase in density, from 1.47 to 1.60 Mg/m³ and from 1.55 to 1.66 Mg/m³, indicating refinement of the pore structure, an increase in AEV, and enhanced capillary retention. With further drying–wetting cycles, the SWRCs shift slightly towards lower suction levels relative to the second drying curve. As the dry densities remain nearly constant beyond the second cycle, the subsequent reduction in water retention behaviour is more likely associated with microstructural degradation induced by repeated drying–wetting, such as microcracking and increased pore network, which reduce capillary efficiency [21-22].

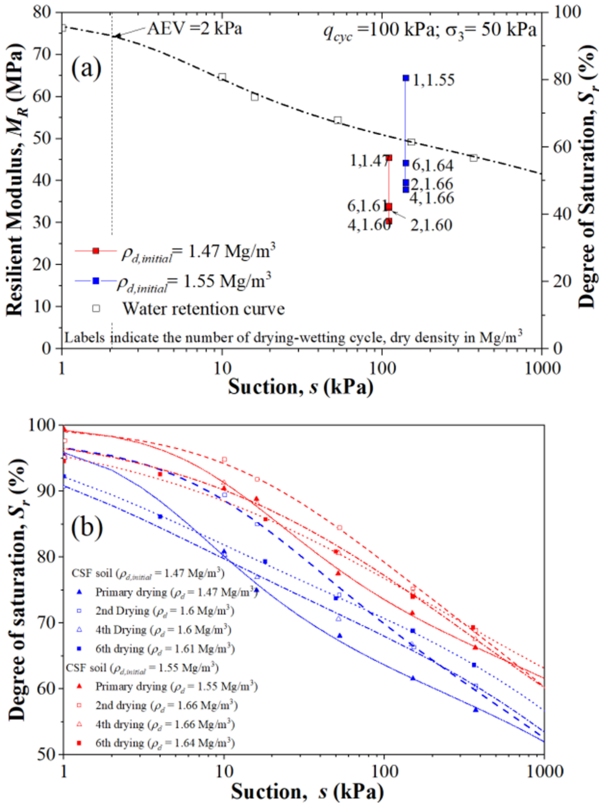

Fig. 4. (a) Effect of dry density and drying–wetting cycles on M_R of CSF (b) SWRCs of CSF with drying–wetting cycles.

Microstructural degradation may occur during drying–wetting cycles which could explain the observed SWRC behaviour. During the initial cycles, this degradation is not pronounced, and overall densification has a more dominant influence, leading to an apparent increase in water retention capacity. However, with further wetting-drying cycles, the effects of microstructural degradation become more pronounced, resulting in a reduction in retention capacity. In contrast, this microstructural degradation influences the resilient modulus from the very first cycle, causing a continuous reduction in M_R despite increasing dry density. This is because resilient modulus is governed by small-strain stiffness and local-scale soil behaviour, which are highly sensitive to microstructural changes such as microcracking and degradation of interparticle contacts.

4 Capability of three existing models

Various models have been proposed to predict M_R of unsaturated soils, ranging from empirical correlations to theoretical frameworks [12-13,19-20]. In this study, three models with different features are evaluated using the experimental data discussed previously.

The first model is the widely used MEPDG (2004) model that describes the variation of M_R with unsaturated conditions using the degree of saturation (S_r). The model is expressed using Equation 1:

$$M_R = 10^{k_s(S_r - S_{opt})} M_{R(\mathrm{opt})} \quad (1)$$

where k_s is the slope obtained from plotting $\log\left(M_{R,exp}/M_{R(opt)}\right)$ against $\left(S_r - S_{r(opt)}\right)$. $M_{R,exp}$ is the measured resilient modulus and $S_{r(opt)}$ denotes the degree of saturation at maximum dry density and optimum water content. The term $M_{R(opt)}$ is defined as $M_{R(opt)} = k_1 p_a \left(\frac{\theta_b}{p_a}\right)^{k_2} \left(\frac{\tau_{oct}}{p_a} + 1\right)^{k_3}$, where θ_b is the bulk stress (kPa), τ_{oct} is the octahedral shear stress (kPa), p_a is the atmospheric pressure (101.3 kPa), and k_1, k_2, and k_3 are fitting parameters.

The second model used is the model proposed by Ng et al. [13] that recognises matric suction as a fundamental stress-state variable in unsaturated soils and explicitly incorporates it into M_R prediction. This model considers suction s and mean net stress p (difference between mean total stress and pore air pressure) as independent stress variables.

This model is expressed using Equation 2:

$$M_R = M_0 \left(\frac{p}{p_r}\right)^{k_1} \left(1+\frac{q_{cyc}}{p_r}\right)^{k_2} \left(1+\frac{s}{p}\right)^{k_3} \quad (2)$$

where M_0 is the resilient modulus at the reference stress state (p = 1 kPa; q_{cyc} = 1 kPa) and zero suction; k_1, k_2, and k_3 are model parameters; and p_r = 1 kPa.

The third model is the model proposed by Azizi et al. [23] in which the effect of both suction and degree of saturation are incorporated in modelling the cyclic behaviour of unsaturated soils. This model is expressed using Equation 3:

$$M_R = \left(\frac{p^*}{p_r}\right)^{k_1} \left(1+\frac{q_{cyc}}{p_r}\right)^{-k_2} + M_0 \exp\left(k_3 \xi\right) \quad (3)$$

where p^* denotes the mean Bishop's stress ($p^* = p + S_r s$); ξ denotes the interparticle bonding parameter ($\xi = (1 - S_r) f_s$, where $f_s = 0.838\, s^{0.06}$); k_1, k_2, and k_3 are model parameters. M_0 represents the saturated resilient modulus at the reference stress state, and p_r is the reference pressure, taken as 1 kPa.

The optimised fitting parameters obtained from calibrating the models are summarised in Table 4. The corresponding coefficient of determination (R^2) for the models are shown in Fig. 5. Although all the models performed well for samples compacted at a given dry density (SM and MTCS), their predictive capability reduced significantly for CSF and GC tested at varying dry densities or subjected to drying-wetting cycles. This suggests that more robust predictive frameworks may be required to improve the ability of these models to provide accurate predictions across the range of soils examined in this study.

Among the evaluated models, the model proposed Azizi et al. [23] is selected for further enhancement as it demonstrated the highest predictive accuracy for the examined experimental data. This improved performance can be attributed to its robust theoretical framework, which incorporates Bishop's stress to combine the effects of suction and degree of saturation, along with a bonding parameter to represent additional normal interparticle forces generated by capillary menisci [24], providing a comprehensive and physically sound description of the partial saturated conditions of the soil. In contrast, the other two models account for the unsaturated state of the soil using either suction or degree of saturation alone. Such representations are inherently limited and may not be sufficiently robust to capture the range of mechanical features observed in unsaturated soils, particularly under cyclic loading where the coupled influence of suction and saturation plays a critical role [23].

5 Proposed model

In order to account for the effects of dry density, this study proposes the following enhanced model:

$$M_R = \left(\frac{p^*}{p_r}\right)^{k_1} \left(1+\frac{q_{cyc}}{p_r}\right)^{k_2} + M_0 \left(\frac{1}{N}\right)^{k_4} \left(\frac{\rho_d}{\rho_{d,max}}\right)^{k_5} \exp\left(k_3 \xi\right) \quad (4)$$

where N is the number of drying–wetting cycles, ρ_d is the dry density, and $\rho_{d,max}$ is the maximum dry density. The proposed model introduces two additional terms relative to the original formulation, together with two additional fitting parameters, k_4 and k_5. The first additional term, $\left(\frac{1}{N}\right)^{k_4}$, is included to capture stiffness degradation associated with drying–wetting cycles due to soil deterioration. The second term, $\left(\frac{\rho_d}{\rho_{d,max}}\right)^{k_5}$, is introduced to represent the effect of the compaction state, expressed as the ratio between the current and the maximum dry density.

When the soil is compacted at maximum dry density ($\rho_d = \rho_{d,max}$) and subjected to a single drying–wetting path ($N = 1$), these two additional terms reduce to unity. Under these conditions, the proposed model simplifies to the original formulation, demonstrating that it is a consistent extension of the original framework. Table 5 presents the fitting parameters and the R^2 values obtained for the studied soils using the proposed model. These R^2 values are compared with those obtained from the other models, as shown in Fig. 5.

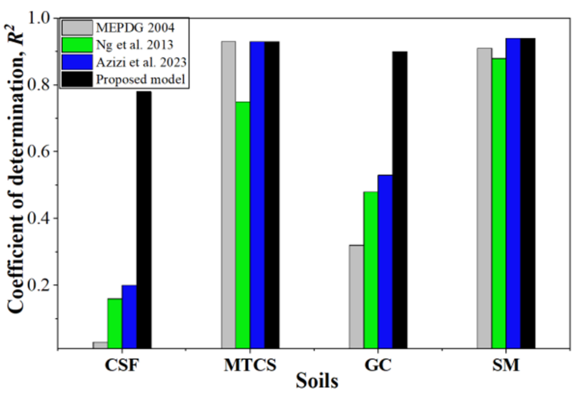

Fig. 5. Comparing R^2 for M_R prediction models.

Table 4. Model parameters and Goodness-of-fit (R²) from the calibration of M_R prediction models.

	MEPDG 2004					Ng et al. 2013					Azizi et al. 2023				
Model Parameters	k_1	k_2	k_3	k_s	R^2	M_0	k_1	k_2	k_3	R^2	M_0	k_1	k_2	k_3	R^2
CSF	0.53	-0.37	0.05	-0.11	0.03	30	0.01	-0.09	0.77	0.16	10	1.2	0.67	1.99	0.2
MTCS	0.19	-0.01	1.68	-0.01	0.93	39.1	0.01	-0.01	1.06	0.75	15.41	0.01	1.82	2.22	0.93
GC	1.36	-2.09	2.58	-0.01	0.32	162	0.01	-0.14	0.14	0.48	105.23	1.01	0.62	0.1	0.53
SM	0.16	-2.31	6	-0.02	0.91	82.34	0.01	-0.02	0.49	0.88	49.8	1.17	0.4	2.09	0.94

Fig. 6 compares the M_R predicted by the newly proposed model with those from existing models, plotted against suction for GC subjected to $q_{cyc} =$ 10 kPa at different densities. The previous models predict either a single curve (Ng et al., 2013) or multiple closely spaced curves (MEPDG and Azizi et al., 2023). In the latter cases, the separation between curves arises from variations in degree of saturation rather than density and therefore does not adequately capture the influence of density on the measured M_R of GC. In contrast, the proposed model produces four clearly distinct curves corresponding to different densities, successfully reflecting density-induced shifts, with M_R decreasing as density decreases.

Table 5. Proposed model parameters and R^2.

Soil	M_0	k_1	k_2	k_3	k_4	k_5	R^2
CSF	20.9	1.09	-0.46	0.01	3	3	0.78
SM	48	1.17	-0.38	2.07	1	0.005	0.94
MTCS	15.8	0.82	-3	2.20	0.01	0.01	0.93
GC	129.8	0.98	-0.51	0.02	0.01	3	0.90

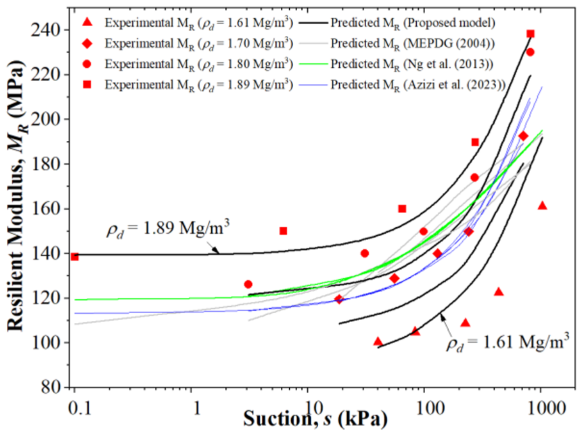

Fig. 6. Comparison of the predicted M_R for GC.

Fig. 7 presents the predicted M_R as a function of the number of drying–wetting cycles, compared with experimental data for CSF subjected to q_{cyc} = 80 kPa at two different densities. The previous models show no appreciable change in M_R with increasing drying–wetting cycles, as they neglect soil deterioration and rely on changes in water retention properties that are not fully representative of stiffness degradation. In contrast, the proposed model explicitly accounts for stiffness degradation induced by drying–wetting cycles, enabling accurate prediction of the observed reduction in M_R. This degradation is consistently captured for both density levels due to the density dependence incorporated in the model, as discussed previously.

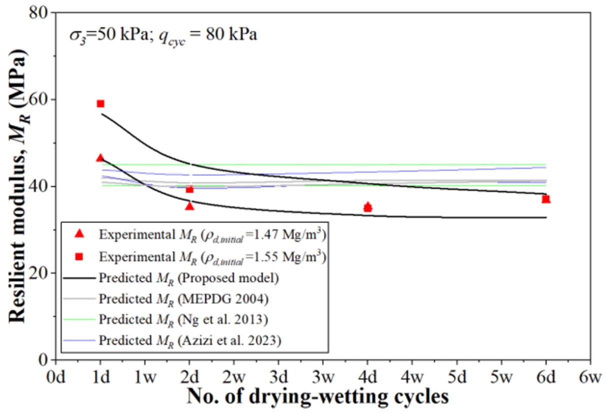

Fig. 7. Comparison of the predicted M_R for CSF.

The proposed model demonstrates consistently an improved agreement across all four soils, achieving higher R^2 values than all the existing models considered here, as shown in Fig. 5. This improvement is particularly pronounced for CSF and GC. When all experimental data used in this study are combined and the predicted resilient modulus is compared with the measured values in Fig. 8, the proposed model shows superior overall performance, achieving an average R^2 value of 0.96, which exceeds that of all the evaluated existing models.

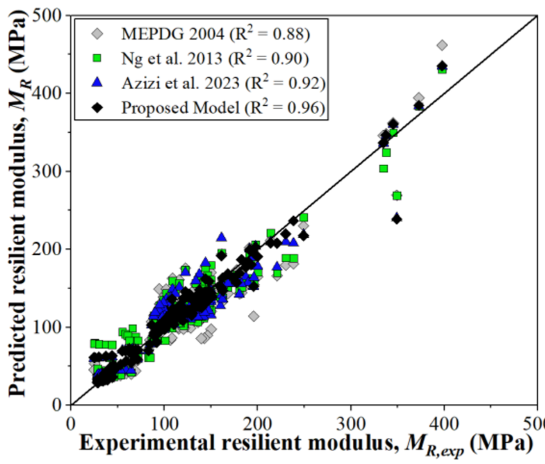

Fig. 8. Comparison of experimental and predicted M_R.

6 Conclusion

This study examined the key factors governing the resilient modulus M_R of various unsaturated soils all relatively high fine fractions. The main findings are:

- M_R increases with increasing suction, with a distinct increase in the rate of this relationship occurring near the soil's air-entry value, highlighting its role in the desaturation process. With increasing cyclic loading, M_R is found to decrease, while the pronounced increase in rate occurs at higher suction levels.

- A decrease in compaction density produces a response similar to that observed under increasing cyclic loading, with a reduction in M_R and a shift in the rate of increase toward higher suction levels. This indicates that in undercompacted soils, particle contacts are less effective, such that higher suction levels are required to mobilise capillary forces and enhance soil stiffness.
- The hysteresis of water retention behaviour results in a non-unique relationship between suction and the degree of saturation, which in turn leads to different resilient modulus values along drying and wetting paths. Furthermore, in some fine-grained soils, repeated drying–wetting cycles can induce soil degradation, leading to a reduction in M_R.
- An assessment of several M_R models showed that frameworks incorporating both suction and degree of saturation offer greater theoretical robustness and predictive capability than those that account for only one of these water retention properties.
- Predictive models that neglect the effect of density or water retention hysteresis do not demonstrate consistent reliability across all density conditions and drying–wetting cycles. To address this limitation, a new model was developed that incorporates soil degradation due to drying–wetting cycles as well as the effects of density variations. This model demonstrated a marked improvement in predictive capability compared with the existing models.

References

1. H.B. Seed, C.K. Chan, C.E. Lee, Resilience characteristics of subgrade soils and their relation to fatigue failures in asphalt pavements. Proc. Int. Conf. Struct. Design Asphalt Pavements, University of Michigan, Ann Arbor, MI, USA, 611–636 (1962)
2. R.G. Hicks, C.L. Monismith, Factors influencing the resilient response of granular materials. Highway Res. Rec. **345**, 15–31 (1971)
3. AASHTO, Standard Specifications for Transportation Materials and Methods of Sampling and Testing, American Association of State Highway and Transportation Officials (2002)
4. A. Kumar, A. Azizi, D.G. Toll, Deterioration of a compacted soil due to suction loss and desiccation cracking. Can. Geotech. J. **62**, 1–18 (2024)
5. C.E. Cary, C.E. Zapata, Resilient modulus for unsaturated unbound materials. Road Mater. Pavement Des. **12**, 615–638 (2011). https://doi.org/10.1080/14680629.2011.9690356
6. D.G. Fredlund, N.R. Morgenstern, R.A. Widger, The shear strength of unsaturated soils. Can. Geotech. J. **15**, 313–321 (1978)
7. S.K. Vanapalli, D.G. Fredlund, D.E. Pufahl, A.W. Clifton, Model for the prediction of shear strength with respect to soil suction. Can. Geotech. J. **33**, 379–392 (1996)
8. Y. Gao, D.A. Sun, Soil-water retention behavior of compacted soil with different densities over a wide suction range and its prediction. Comput. Geotech. **91**, 17–26 (2017)
9. Wheeler SJ, Sharma RS, Buisson MSR (2003) Coupling of hydraulic hysteresis and stress–strain behaviour in unsaturated soils. Géotechnique **53**(1):41–54
10. Lloret-Cabot M, Wheeler SJ, Sánchez M (2017) A unified mechanical and retention model for saturated and unsaturated soil behaviour. Acta Geotech **12**(1):1–21
11. Lloret-Cabot M, Wheeler SJ, Pineda J, Romero E and Sheng D (2018) From saturated to unsaturated conditions and vice versa. Acta Geotech **13**(1):15–37
12. S. Gupta, A. Ranaivoson, T. Edil, C. Benson, Predictive model for the resilient modulus of unsaturated subgrade soils. Proc. FAA Worldwide Airport Technol. Transfer Conf., Atlantic City, NJ, USA (2007)
13. C.W.W. Ng, C. Zhou, Q. Yuan, J. Xu, Resilient modulus of unsaturated subgrade soil: Experimental and theoretical investigations. Can. Geotech. J. **50**, 223–232 (2013)
14. C.N. Khoury, N.N. Khoury, G.A. Miller, Effect of cyclic suction history (hydraulic hysteresis) on resilient modulus of unsaturated fine-grained soil. Transp. Res. Rec. **2232**, 68–75 (2011)
15. J. Zhang, J. Peng, W. Liu, W. Lu, Predicting resilient modulus of fine-grained subgrade soils considering relative compaction and matric suction. Road Mater. Pavement Des. **22**, 703–715 (2021)
16. J.H.C. Everton, S. Erlingsson, Characterising the resilient behaviour of unsaturated sandy soils under suction-controlled tests. Road Mater. Pavement Des. **27**, 102–124 (2026). https://doi.org/10.1080/14680629.2025.2480249
17. G. Cai, X. Yang, B. Han, Y. Su, H. Wang, F. Li, Influence of drying–wetting cycles on the structure and dynamic characteristics of unsaturated clays: an experimental study. Can. Geotech. J. **62**, 1–15 (2025). https://doi.org/10.1139/cgj-2024-0275
18. D.G. Fredlund, A. Xing, Equations for the soil–water characteristic curve. Can. Geotech. J. **31**, 521–532 (1994)
19. ARA Inc., ERES Consultants Division, Guide for Mechanistic-Empirical Design of New and Rehabilitated Pavement Structures, NCHRP Project 1-37A (Transportation Research Board, Washington DC, 2004)
20. A. Azizi, A. Kumar, D.G. Toll, Coupling cyclic and water retention response of a clayey sand subjected to traffic and environmental cycles. Géotechnique **73**, 401–417 (2023). https://doi.org/10.1680/jgeot.21.00063
21. G. Musso, A. Azizi, C. Jommi, A microstructure-based elastoplastic model to describe the behaviour of a compacted clayey silt in isotropic and triaxial compression. Can. Geotech. J. **57**, 1025–1043 (2020)
22. A. Azizi, G. Musso, C. Jommi, R.M. Cosentini, Evolving fabric and its impact on the shearing behaviour of a compacted clayey silt exposed to drying–wetting cycles, in Proc. 7th Int. Conf. Unsaturated Soils (UNSAT2018), Hong Kong (2018), pp. 641–646

23. A. Azizi, A. Kumar, D.G. Toll, The bounding effect of the water retention curve on the cyclic response of an unsaturated soil. Acta Geotech **18**, 1901–1917 (2023)
24. D. Gallipoli, A. Gens, R. Sharma, J. Vaunat, An elasto-plastic model for unsaturated soil incorporating the effects of suction and degree of saturation on mechanical behaviour. Géotechnique **53**, 123–135 (2003)